Electronic Structures and Spectra of Trinuclear Carbonyl Complexes

David R. Tyler, Robert A. Levenson, and Harry B. Gray*

Contribution No. 5789 from the Arthur Amos Noyes Laboratory of Chemical Physics, California Institute of Technology, Pasadena, California 91125. *Received May 17, 1978*

Abstract: Detailed experimental studies of the electronic spectra of trinuclear metal carbonyls have been made. An extended Hückel molecular orbital calculation on D_{3h} $Ru_3(CO)_{12}$ has been performed to aid in assigning the spectra of the triangular cluster complexes. A band at 390 nm (2.56 μm^{-1}) in the spectrum of $Ru_3(CO)_{12}$ is polarized in the plane of the Ru_3 triangle, exhibits an MCD A term, and blue shifts and sharpens on cooling to 77 K. This band is assigned to the $^1A_1' \rightarrow {}^1E'$ (xz (bonding) $\rightarrow xz$ (antibonding)), or $\sigma \rightarrow \sigma^*$ transition. A weak band at 320 nm (3.12 μm^{-1}) is assigned to the $^1A_1' \rightarrow {}^1E'$ (z^2 (antibonding) $\rightarrow xz$ (antibonding)), or $\sigma^{*\prime} \rightarrow \sigma^*$ transition. Similar evidence suggests that bands at 330 (3.03 μm^{-1}) and 385 nm (2.60 μm^{-1}) in the spectrum of $Os_3(CO)_{12}$ be assigned to $\sigma \rightarrow \sigma^*$ and $\sigma^{*\prime} \rightarrow \sigma^*$ transitions, respectively. The relative energies of the $\sigma \rightarrow \sigma^*$ and $\sigma^{*\prime} \rightarrow \sigma^*$ transitions in the $M_3(CO)_{12}$, $Ru_3(CO)_9(PR_3)_3$, and $Fe_nRu_{3-n}(CO)_{12}$ (n = 0–3) molecules depend on the ligand field splitting of the xz and z^2 orbitals in the corresponding $M(CO)_4$ and $Ru(CO)_3PR_3$ fragments. A single crystal polarized spectrum of $Fe_3(CO)_{12}$ shows that the two lowest energy bands at 602 and 437 nm (1.66 and 2.29 μm^{-1}) are polarized in the plane of the Fe_3 triangle. These bands are assigned to the $\sigma^{*\prime} \rightarrow \sigma^*$ and $\sigma \rightarrow \sigma^*$ transitions, respectively. Intense bands (ϵ_M >25 000) at approximately 4.0 μm^{-1} are assigned to MLCT transitions in the $M_3(CO)_{12}$ molecules. An MO scheme for the D_{4h} molecules $M_2Fe(CO)_{14}$ (M = Mn, Re) is presented. The lowest energy allowed transition in each of these molecules is predicted to be of the metal-metal σ to σ^* type ($^1A_{1g} \rightarrow {}^1A_{2u}$ ($a_{2u} \rightarrow 2a_{1g}$)). The lowest energy band in the spectrum of $Re_2Fe(CO)_{14}$ (2.63 μm^{-1}) is polarized along the ReFeRe axis, consistent with the $^1A_{1g} \rightarrow {}^1A_{2u}$ assignment.

Previous work on the electronic spectra of dimanganese decacarbonyl and related species has shown that the lowest energy absorption bands are attributable to $\sigma \rightarrow \sigma^*$ and $d\pi \rightarrow \sigma^*$ transitions, with the σ and σ^* orbitals being the bonding and antibonding metal $d\sigma$ (mainly d_{z^2}) combinations.[1] Excitation of $\sigma \rightarrow \sigma^*$ has been shown to dictate the photochemistry of these complexes, by inducing homolytic cleavage of the metal-metal bond.[2] Our interest in the photochemistry of larger carbonyl clusters has led us to investigate the electronic structures of $M_3(CO)_{12}$ (M = Fe, Ru, Os) and $M_2Fe(CO)_{14}$ (M = Mn, Re) molecules. As photofragmentation of $Ru_3(CO)_{12}$ has been reported,[3] it was of interest to us to determine whether low-lying electronic transitions similar to $\sigma \rightarrow \sigma^*$ in binuclear carbonyls would be observed in these larger clusters. Herein we report the results of our electronic spectral studies on several trinuclear carbonyl clusters. Extended Hückel molecular orbital calculations were performed on the $Ru(CO)_4$ fragment and the $Ru_3(CO)_{12}$ molecule to aid in the interpretation of the spectra.

Experimental Section

$Fe_3(CO)_{12}$, $Ru_3(CO)_{12}$, and $Os_3(CO)_{12}$ were purchased from Strem Chemical Co. $Fe_3(CO)_{12}$ was purified by sublimation at 60 °C. $Ru_3(CO)_{12}$ was recrystallized from toluene. $Os_3(CO)_{12}$ was recrystallized from benzene and then washed dry with ether.

$Ru(CO)_5$,[3] $Ru_3(CO)_9(PPh_3)_3$,[4,5] $Ru_3(CO)_9(PEtPh_2)_3$,[4,5] $Fe_2Ru(CO)_{12}$,[6] $FeRu_2(CO)_{12}$,[6] $(PPN)MnFe_2(CO)_{12}$,[7] $Mn_2Fe(CO)_{14}$,[8] $MnFeRe(CO)_{14}$,[9] $Re_2Fe(CO)_{14}$,[10] and $Fe_2(CO)_9$[11] were prepared by standard methods.

Electronic absorption and MCD spectra were measured on Cary 17 and Cary 61 instruments. Spectra at 77 K were obtained as described previously;[1] for some measurements a Cryogenic Technology, Inc., Model 21 cryocooler was employed. The contraction of 2-methylpentane at 77 K was measured to be 22% relative to 300 K. The use of EPA and 3-PIP as glassing solvents has been described previously.[1] All the low-temperature spectra reported in this paper are uncorrected for solvent contraction. Techniques for obtaining band polarizations using the nematic liquid crystal solvent BPC have been described previously.[12]

Thin single crystals of $Fe_3(CO)_{12}$ were grown from hexane on quartz plates. The crystals are strongly dichroic, being green in one orientation and colorless in the other. Polarized spectra were measured along the extinction directions of the crystal face. A polarized infrared spectrum was used to obtain the orientation of the $Fe_3(CO)_{12}$ molecules in the crystals. For the infrared measurements, crystals were grown on sapphire plates. Dahl and Rundle have reported[13] the polarized infrared spectrum of $Fe_3(CO)_{12}$. We found that their "$\parallel$ to b" corresponded to our colorless orientation and their "$\parallel$ to C_B" to our green orientation. The orientation of the molecules in the unit cell is such that the plane of the Fe_3 triangle is nearly perpendicular to b. Thus, the green orientation is for polarized light with the electric vector in the plane of the Fe_3 triangle and the colorless orientation for the electric vector perpendicular to the Fe_3 plane.

Molecular Orbitals for $Ru(CO)_4$ and $Ru_3(CO)_{12}$

The molecular orbital energy levels for $Ru(CO)_4$ were calculated using an iterative, extended-Hückel (F = 2) procedure.[14] The coordinate system used is shown in Figure 1. The geometry of the fragment was idealized to C_{2v} symmetry with the angle C(1)-Ru-C(2) equal to 180° and all Ru-C-O angles also equal to 180°. The value of 100° for the angle C(3)-Ru-C(4) was taken from a crystal structure determination of $Ru_3(CO)_{12}$.[15] The bond lengths used were $Ru-C_{eq}$ = 1.93 Å, $Ru-C_{ax}$ = 1.89 Å, and C-O = 1.14 Å, where eq and ax refer to equatorial and axial, respectively. These values were taken from the mean bond lengths reported for $Ru_3(CO)_{12}$.[15]

The CO ligand basis set consisted of the filled 4σ, 5σ, 1π, and the unfilled 2π molecular orbitals.[14] These functions were taken from SCF calculations.[16] Slater atomic orbitals were used for the carbon and oxygen atomic basis set.[16] The 4d, 5s, and 5p Ru atomic orbitals were taken from an earlier paper.[17]

The results of the $Ru(CO)_4$ calculation are presented on the left-hand side of the scheme in Figure 2.[18] Similar results have been obtained[19] in a calculation of the molecular orbitals of $Mn(CO)_4$. The $Ru(CO)_4$ calculation shows that there are three low-lying d orbitals that are relatively unaffected by the four CO ligands. These orbitals are directed between the ligands. Several lobes of the xz orbital are directed toward the equatorial ligands. The higher energy of this orbital reflects this antibonding character. The remaining d orbital, the $x^2 - y^2$, is directed at the axial CO ligands and, as a result, possesses extreme antibonding character. The $x^2 - y^2$ orbital is above some of the CO π^* orbitals, and it is not shown in Figure 2. The lowest unoccupied MO is a hybrid (15% $x^2 - y^2$, 25% z, 45% π^*) and is of a_1 symmetry in $Ru(CO)_4$. This orbital is involved

0002-7863/78/1500-7888$01.00/0

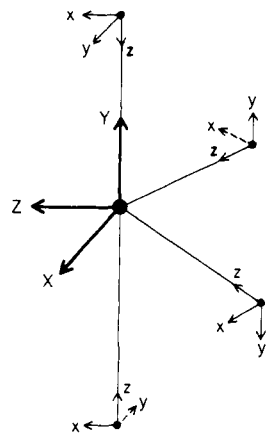

Figure 1. The coordinate system for the $Ru(CO)_4$ fragment.

Table I. Selected Eigenvalues of $Ru_3(CO)_{12}$

$-E$, μm^{-1}	symmetry	orbital character
3.27	e′	π^*
3.39	a_1'	π^*
3.60	e′	π^*
4.98 (LUMO)	a_2'	xz (σ^*)
6.77 (HOMO	a_1'	x^2-y^2, z, π^*
7.14	e″	yz
7.18	e′	z^2 ($\sigma^{*\prime}$)
7.20	a_1''	xy
7.41	e″	xy
7.50	e′	xz (σ)
7.73	a_2''	yz
8.32	a_1'	z^2 (σ')
10.71	a_1'	σ

in the metal-metal bond network when the $Ru(CO)_4$ fragments combine to form $Ru_3(CO)_{12}$.

The RuRu bond distance in $Ru_3(CO)_{12}$ was taken to be 2.848 Å.[15] The F parameters used were $F_{M\sigma} = F_{\sigma\sigma} = 1.50$, $F_{M\pi} = F_{\pi\pi} = 2.2$, $F_{\sigma,\pi} = F_{MM} = 2.0$, i.e., the same used for $Mn_2(CO)_{10}$.[1] Corrections were applied[1] to the metal orbital H_{ii} values. The calculation was not iterative owing to program limitations. Thus, VSIE values for the metal H_{ii} were adjusted to those from a charge-iterative calculation on $Mo(CO)_6$.[14] These values are $d = -7.4$, $s = -6.4$, and $p = -3.5$ μm^{-1}.

A partial listing of the eigenvalues from the calculation is given in Table I. These results are represented as an MO scheme in Figure 2. The metal orbitals in the cluster have been identified by their d orbital parentage because these basis set orbitals remain relatively unmixed in the cluster. The predicted ground state is $^1A_1'$ ($a_1'^2$), which accords with the diamagnetism of the compound.[20]

The energy levels of the metal orbitals in the $Ru_3(CO)_{12}$ cluster are determined mainly by their energies in the $Ru(CO)_4$ fragment (Figure 2). Every d atomic basis orbital in the fragment can be combined into an a-type and an e-type basis set of molecular orbitals in the cluster. Depending upon the d orbital involved, one of these molecular orbitals will be bonding and the other antibonding with respect to the metal-metal interaction. The a_1 LUMO in $Ru(CO)_4$ forms a bonding a_1' orbital in $Ru_3(CO)_{12}$; this orbital is occupied in the ground state of the trinuclear carbonyl and accounts for a significant fraction of the metal-metal bonding. The following notation is introduced to simplify the electronic spectral discussion. By analogy to $Mn_2(CO)_{10}$,[1] the e′ (xz) bonding orbital is σ, whereas the a_2' (xz) antibonding orbital is σ^* (σ^* is the LUMO

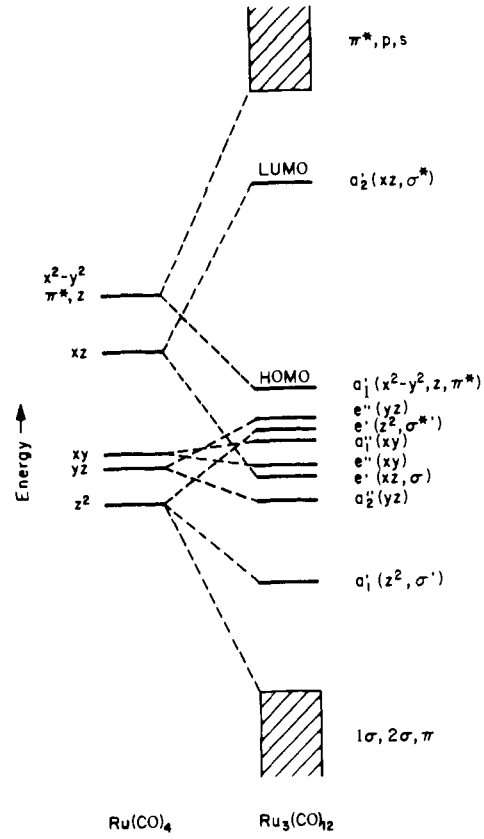

Figure 2. MO scheme for $Ru_3(CO)_{12}$. Selected energy levels for the $Ru(CO)_4$ fragment are shown at left (the $Ru(CO)_4$ HOMO is xz, and the LUMO is π^*,z).

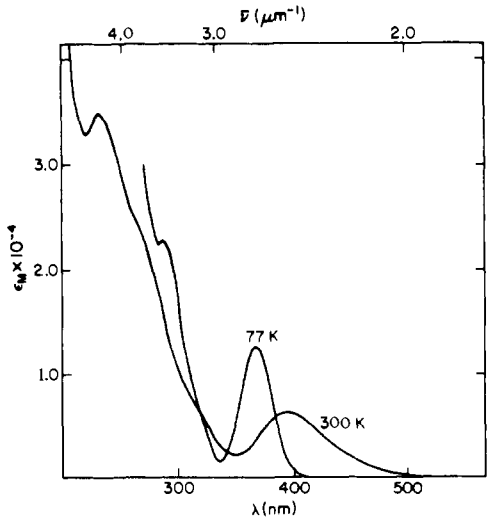

Figure 3. Electronic absorption spectra of $Ru_3(CO)_{12}$ in 2-methylpentane at 300 and 77 K.

in $Ru_3(CO)_{12}$); the a_1' (z^2) bonding orbital is σ' and the e′ (z^2) antibonding orbital is $\sigma^{*\prime}$. There are three allowed one-electron transitions from the d block of molecular orbitals to σ^*: $\sigma \rightarrow \sigma^*$ ($^1A_1' \rightarrow {}^1E'$), $\sigma^{*\prime} \rightarrow \sigma^*$ ($^1A_1' \rightarrow {}^1E'$) and $a_1''(xy) \rightarrow \sigma^*(^1A_1' \rightarrow {}^1A_2'')$.

Electronic Spectra

The electronic spectra of $Ru_3(CO)_{12}$ at 300 and 77 K are shown in Figure 3. The most interesting feature is an intense band at 390 nm (2.56 μm^{-1}) that sharpens and blue shifts markedly upon cooling. In the nematic liquid crystal solvent

Table II. Electronic Spectral Data[a] and Transition Assignments

complex	300 K			77 K				MCD	
	λ_{max}, nm	$\bar{\nu}_{max}$, μm^{-1}	$\epsilon_M \times 10^{-4}$	λ_{max}, nm	$\bar{\nu}_{max}$, μm^{-1}	$\epsilon_M \times 10^{-4}$	polarization	A term	assignment
$Ru_3(CO)_{12}$	390	2.56	0.64	367	2.72	1.02	in-plane[b]	379	$\sigma \rightarrow \sigma^*$
	320 sh	3.12		320 sh	3.12			305	$\sigma^{*\prime} \rightarrow \sigma^*$
				292	3.42	1.50			
	270 sh	3.70							
	238	4.20	3.50						MLCT
$Os_3(CO)_{12}$	385 sh	2.60	0.36	381	2.62	0.56		385	$\sigma^{*\prime} \rightarrow \sigma^*$
	330	3.03	0.86	317	3.15	2.06		327	$\sigma \rightarrow \sigma^*$
	280 sh	3.57		275 sh	3.64	1.30			
	240	4.17	2.48						MLCT
$Fe_3(CO)_{12}$	602	1.66	0.32	605	1.65	0.52	in-plane		$\sigma^{*\prime} \rightarrow \sigma^*$
	437 sh	2.29		435	2.30	0.48	in-plane		$\sigma \rightarrow \sigma^*$
	360 sh	2.78		360 sh	2.78				
	310 sh	3.22		320 sh	3.12				
				297	3.37	1.85			
	263	3.80	3.00						MLCT
$FeRu_2(CO)_{12}$	470 sh	2.13		468	2.17	0.70			$\sigma^{*\prime} \rightarrow \sigma^*$
	390	2.56	0.88	368	2.72	1.28			$\sigma \rightarrow \sigma^*$
$Ru_3(CO)_9(PEtPh_2)_3$[c]	492	2.03	1.15	495	2.02	1.59		487	$\sigma^{*\prime} \rightarrow \sigma^*$
	370	2.70	1.22	353	2.83	1.54		372	$\sigma \rightarrow \sigma^*$
$Ru_3(CO)_9(PPh_3)_3$[c]	507	1.97	1.23	520	1.92	1.88		501	$\sigma^{*\prime} \rightarrow \sigma^*$
	387	2.58	1.28	375	2.67	2.00		394	$\sigma \rightarrow \sigma^*$
$Mn_2Fe(CO)_{14}$[d]	431	2.32	2.38	424	2.36	4.01			$\sigma \rightarrow \sigma^*$
$Re_2Fe(CO)_{14}$	380	2.63	3.00	379	2.64	4.82	ReFeRe axis		$\sigma \rightarrow \sigma^*$
$MnFeRe(CO)_{14}$	403	2.48							$\sigma \rightarrow \sigma^*$
$Ru(CO)_5$	260 sh	3.85	0.57						$e' \rightarrow a'_1$
	236	4.24	0.84						MLCT

[a] In 2-methylpentane unless noted otherwise. [b] R. A. Levenson, Ph.D. Thesis, Columbia University, 1970. [c] In EPA. [d] In 3-PIP.

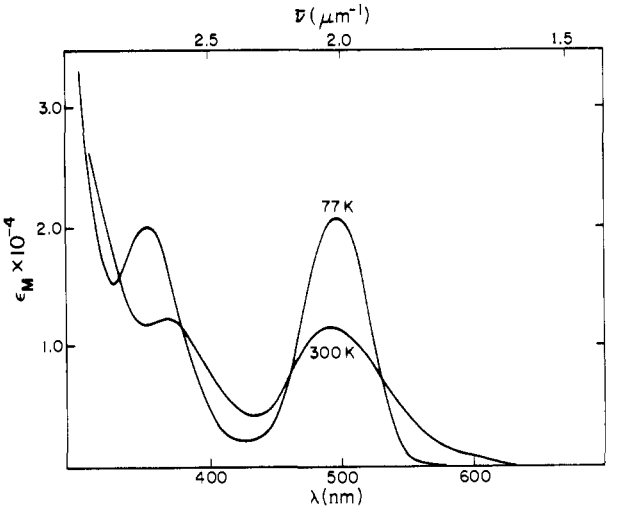

Figure 4. Electronic absorption spectra of $Ru_3(CO)_9(PEtPh_2)_3$ in EPA at 300 and 77 K.

BPC, the 2.56-μm^{-1} band is in-plane (X-Y) polarized (Table II). This means that the transition must be either $\sigma \rightarrow \sigma^*$ or $\sigma^{*\prime} \rightarrow \sigma^*$, either of which gives an E′ excited state and is thus X-Y polarized. The A term in the MCD spectrum of this band confirms the degeneracy of the excited state (Table II). According to the calculation, the $\sigma^{*\prime}$ orbital is higher in energy than the σ orbital (Figure 2). However, the calculated energy separation between the $\sigma^{*\prime}$ and σ orbitals is too small (0.32 μm^{-1}) to predict with any confidence which of the $^1A_1' \rightarrow {}^1E'$ transitions lies to lower energy. In order to decide this question, we found it necessary to examine the spectra of several closely related derivatives.

The spectra of $Ru_3(CO)_9(PEtPh_2)_3$ at 300 and 77 K are shown in Figure 4. Spectral data for other $Ru_3(CO)_9(PR_3)_3$ complexes are given in Table II. All these complexes have bands near 390 nm (~2.5 μm^{-1}) that sharpen and blue shift on cooling. But, unlike $Ru_3(CO)_{12}$, the phosphine-substituted complexes have an additional band near 500 nm (~2.0 μm^{-1}). Since phosphine substitution occurs at a site that is in the Ru_3 plane, it is the energy of the xz orbital that is primarily affected (Figure 5). Replacement of CO by a phosphine makes the xz orbital less antibonding. This means that the xz-z^2 energy separation in the $Ru(CO)_3(PR_3)$ fragment will be less than in the $Ru(CO)_4$ fragment. As a result of the decreased separation, when the fragments combine to form the trimer, the z^2 antibonding orbital ($\sigma^{*\prime}$) is higher in energy than the xz bonding orbital. Thus the energy of the $\sigma^{*\prime} \rightarrow \sigma^*$ transition should decrease on going from $Ru_3(CO)_{12}$ to $Ru_3(CO)_9(PR_3)_3$. Accordingly, the "new" band at ~2.0 μm^{-1} in the $Ru_3(CO)_9(PR_3)_3$ complexes is assigned to the $\sigma^{*\prime} \rightarrow \sigma^*$ transition. Both the ~2.0 and ~2.6 μm^{-1} bands exhibit MCD A terms (Figure 6), which is consistent with our assignment.

The above interpretation of the $Ru_3(CO)_9(PR_3)_3$ spectrum suggests an assignment for the 2.56-μm^{-1} band in $Ru_3(CO)_{12}$. In addition to having nearly the same energy, this band has the same temperature-dependent behavior (sharpening and blue shifting on cooling) as the ~2.6-μm^{-1} band in the $Ru_3(CO)_9(PR_3)_3$ complexes. These similarities suggest that the same transition is involved in each case and hence the 2.56-μm^{-1} band is assigned to $\sigma \rightarrow \sigma^*$ in the $Ru_3(CO)_{12}$ molecule. We note that this $\sigma \rightarrow \sigma^*$ assignment is consistent with the interpretation of the spectra of binuclear metal carbonyls.[1] The observed temperature dependence of the band shape in $M_2(CO)_{10}$ molecules is related to the substantial depopulation of excited M_2 vibrational levels that occurs upon cooling the molecule to 77 K.[1] Similar temperature-dependent behavior is expected for $\sigma \rightarrow \sigma^*$ bands in trinuclear clusters, as the electronic transition will be coupled to the low-frequency M_3 stretching motions in these molecules.

Phosphine substitution lowers the energy of the $\sigma \rightarrow \sigma^*$ transition in $Mn_2(CO)_{10}$. Thus, it is possible that the band assignments above are reversed, that is, phosphine substitution has shifted the $\sigma \rightarrow \sigma^*$ transition from 2.56 μm^{-1} in $Ru_3(CO)_{12}$ to ~2.00 μm^{-1} in $Ru_3(CO)_9(PR_3)_3$. Two lines of evidence

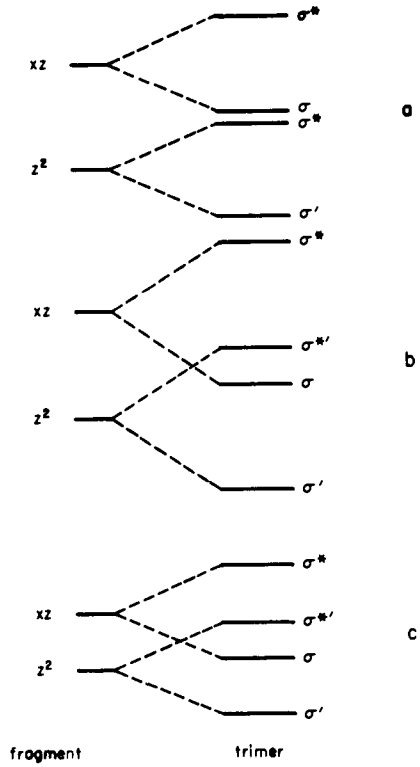

Figure 5. Schematic of the interactions of xz and z^2 fragment orbitals to form trimer cluster orbitals ($\sigma',\sigma^{*\prime},\sigma,\sigma^*$): (a) proposed interaction scheme for $Ru_3(CO)_{12}$; (b) the effect of increased metal-metal overlap on the σ and $\sigma^{*\prime}$ orbital energies, as proposed for $Os_3(CO)_{12}$; and (c) the effect of decreased z^2–xz energy separation on the σ and $\sigma^{*\prime}$ orbital energies, as proposed for $Ru_3(CO)_9(PR_3)_3$.

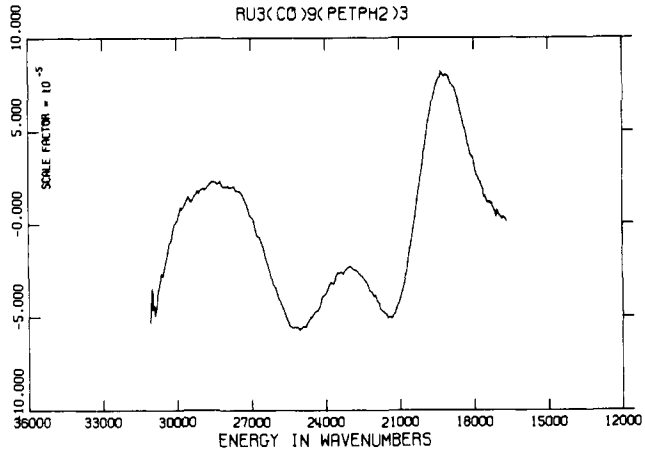

Figure 6. MCD spectrum of $Ru_3(CO)_9(PEtPh_2)_3$ in 2-methylpentane at 25 °C. The ordinate is in units of ellipticity G^{-1}. 10^4 wavenumbers (cm^{-1}) = 1 μm^{-1}.

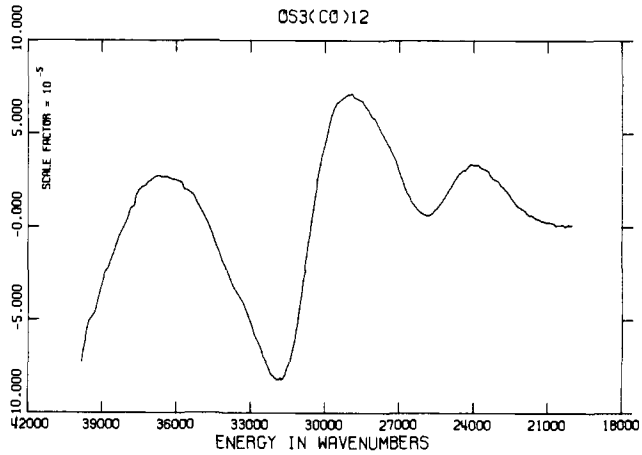

Figure 7. MCD spectrum of $Os_3(CO)_{12}$ in 2-methylpentane at 25 °C. The ordinate is in units of ellipticity G^{-1}. 10^4 wavenumbers (cm^{-1}) = 1 μm^{-1}.

suggest that the latter has not happened. Firstly, the shifts in the $Mn_2(CO)_{10}$ $\sigma\rightarrow\sigma^*$ transition energy with phosphine substitution are much smaller than 0.56 μm^{-1} (2.56-2.00 μm^{-1}). Secondly, on cooling, the ~2.6-μm^{-1} band sharpens and blue shifts, as is characteristic of a $\sigma\rightarrow\sigma^*$ transition.

Spectra of several $Ru_3(CO)_9(ER_3)_3$ (E = P, As, Sb) derivatives show that the lowest band increases in energy according to $PPh_3 < PEtPh_2 < PEt_2Ph < PEt_3$ (and also $PPh_3 < AsPh_3 < SbPh_3$),[5] following the σ-donor ability of the ligands. With increasing σ-donor ability, the d_{z^2}–d_{xz} ligand field splitting increases in any given monomeric fragment, with a corresponding increase in energy for the $\sigma^{*\prime}\rightarrow\sigma^*$ transition in the trimer. We also note that the colors of the compounds $M_3(CO)_{11}PR_3$, $M_3(CO)_{10}(PR_3)_2$, and $M_3(CO)_9(PR_3)_3$ (M = Ru, Os) are generally yellow, orange, and red, respectively.[21] Increasing phosphine substitution likely results in a decrease in the average d_{z^2}–d_{xz} (fragment) ligand field splitting, thereby lowering the energy of the $\sigma^{*\prime}\rightarrow\sigma^*$ transition in the trinuclear molecules.

Electronic absorption spectral data for $Os_3(CO)_{12}$ are summarized in Table II. The peak at 330 nm (3.03 μm^{-1}) and the shoulder at 385 nm (2.60 μm^{-1}) give rise to MCD A terms (Figure 7), indicating degenerate excited states. The band at 3.03 μm^{-1} sharpens and blue shifts, and is assigned to $\sigma\rightarrow\sigma^*$. The weaker band at 2.60 μm^{-1} is assigned to $\sigma^{*\prime}\rightarrow\sigma^*$, which is the other low-lying transition to a degenerate excited state.

The $\sigma\rightarrow\sigma^*$ transition was assigned to the lowest energy band in $Ru_3(CO)_{12}$; however, in $Os_3(CO)_{12}$, the $\sigma^{*\prime}\rightarrow\sigma^*$ transition is below $\sigma\rightarrow\sigma^*$. We suggest that this pattern of relative transition energies is reasonable because the metal-metal orbital interactions should be greater in $Os_3(CO)_{12}$ than in $Ru_3(CO)_{12}$, causing a greater bonding-antibonding energy splitting in the former molecule. As a result, in $Os_3(CO)_{12}$ the z^2 antibonding MO ($\sigma^{*\prime}$) moves above the xz bonding orbital (σ), as shown in Figure 5b, and the $\sigma\rightarrow\sigma^*$ transition occurs at higher energy ($Ru_3(CO)_{12}$, 2.56 μm^{-1} < $Os_3(CO)_{12}$, 3.05 μm^{-1}). The $\sigma^{*\prime}\rightarrow\sigma^*$ transition therefore falls at lower energy than $\sigma\rightarrow\sigma^*$ in $Os_3(CO)_{12}$. Independent evidence that the metal-metal interactions are stronger in $Os_3(CO)_{12}$ than in $Ru_3(CO)_{12}$ comes from stretching force constants, which are 0.91 mdyn/Å for the former molecule and 0.82 mdyn/Å for the latter.[22] A similar correlation of $\sigma\rightarrow\sigma^*$ transition energies and stretching force constants has been noted[1] for $M_2(CO)_{10}$ (M = Mn, Tc, Re) molecules.

The spectral data for $Os_3(CO)_{12}$ show that the $\sigma^{*\prime}\rightarrow\sigma^*$ band is much weaker than that associated with the $\sigma\rightarrow\sigma^*$ transition. Careful inspection of the $Ru_3(CO)_{12}$ spectrum reveals a weak band, which appears as a shoulder at 3.12 μm^{-1}, and the MCD spectrum of the molecule (Table II) indicates the presence of an A term positioned at 305 nm (3.20 μm^{-1}). We propose, therefore, that the weak band at 3.12 μm^{-1} in $Ru_3(CO)_{12}$ is attributable to $\sigma^{*\prime}\rightarrow\sigma^*$.

We turn next to the spectrum of $FeRu_2(CO)_{12}$, which possesses a triangular $FeRu_2$ cluster and only terminal CO groups in solution.[6] A band at 390 nm (2.56 μm^{-1}) in the spectrum of this molecule (Table II) blue shifts and sharpens upon cooling. Owing to this characteristic temperature-dependent behavior, this band is assigned to the $\sigma\rightarrow\sigma^*$ transition. The weaker band at 470 nm (2.13 μm^{-1}) is assigned to the $\sigma^{*\prime}\rightarrow\sigma^*$

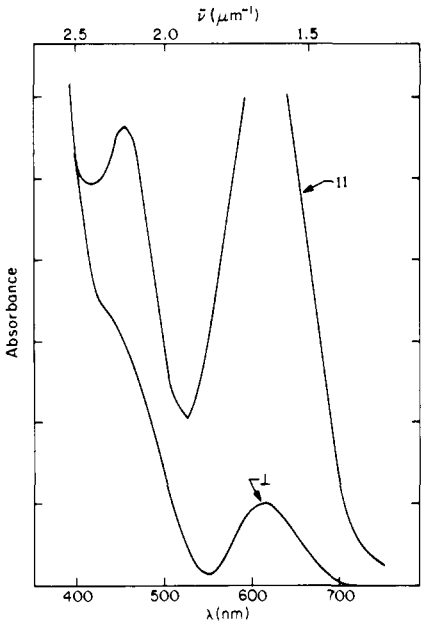

Figure 8. Single crystal polarized electronic absorption spectra of $Fe_3(CO)_{12}$ at 25 °C. The spectra are for the electric vector of light perpendicular to the Fe_3 plane ($\perp$) and in the plane ($\parallel$).

transition. The presence of Fe in the $FeRu_2$ triangle decreases the average ligand field splitting of the xz and z^2 orbitals (Figure 5c), thereby placing the $\sigma^{*\prime}$ orbital above σ, as in the case of $Ru_3(CO)_9L_3$. Consequently, the $\sigma^{*\prime}\rightarrow\sigma^*$ transition falls lower than $\sigma\rightarrow\sigma^*$.

Electronic absorption spectral data for $Fe_3(CO)_{12}$ are given in Table II. If the symmetry of CO-bridged $Fe_3(CO)_{12}$ is idealized to C_{2v}, then the $\sigma\rightarrow\sigma^*$ and $\sigma^{*\prime}\rightarrow\sigma^*$ (both $e' \rightarrow a_2'$) transitions are no longer $^1A' \rightarrow {}^1E'$, but are split into two transitions, $^1A_1 \rightarrow {}^1A_1$ and $^1A_1 \rightarrow {}^1B_1$. Both transitions are polarized in the plane of the triangle, one component of each in the Z (C_{2v}) direction ($^1A_1 \rightarrow {}^1A_1$) and the other in the X (C_{2v}) direction ($^1A_1 \rightarrow {}^1B_1$). Spectroscopic measurements on a single crystal of $Fe_3(CO)_{12}$ clearly show that the two lowest energy bands are polarized in the plane of the Fe_3 triangle (Figure 8). Dahl and Rundle have discussed the disordering of the $Fe_3(CO)_{12}$ molecules in the unit cell.[13] It is this disorder that prevents us from distinguishing the Z and X polarizations. However, even our glass spectra at 77 K revealed no splitting of either the 602- (1.66) or the 437-nm (2.29 μm^{-1}) band.

As in the other $M_3(CO)_{12}$ molecules and consistent with the polarization data, we assign the lowest energy bands in $Fe_3(CO)_{12}$ to the $\sigma\rightarrow\sigma^*$ and $\sigma^{*\prime}\rightarrow\sigma^*$ transitions. However, it is possible that one or both of these bands are low-energy charge transfer transitions involving the bridging CO ligands. To examine this possibility, we studied the electronic spectrum of $Fe_2(CO)_9$, a molecule with three bridging CO groups. The spectrum showed only rising absorption into the UV with no bands of appreciable intensity in the visible region. Likewise, our study of the electronic spectrum of $Co_2(CO)_8$ did not reveal any bands in the visible region attributable to metal $\rightarrow$ bridging-CO transitions.[23] Further evidence that the two low-energy transitions in $Fe_3(CO)_{12}$ are not charge transfer is provided by the spectrum of $(PPN)MnFe_2(CO)_{12}$. The cluster structure of $MnFe_2(CO)_{12}^-$ is the same[7] as that of $Fe_3(CO)_{12}$. The spectra of the two complexes are similar except that the two lowest energy transitions in $MnFe_2(CO)_{12}^-$ (1.74, 2.86 μm^{-1}) are blue shifted with respect to their counterparts in $Fe_3(CO)_{12}$ (1.66, 2.29 μm^{-1}). Substitution of Mn^- for Fe(0) should red shift metal to ligand charge transfer (MLCT) transitions. Such a shift has been observed for the MLCT transitions when Cr^- is substituted for Mn(0) in $Mn_2(CO)_{12}$.[1] Thus it is unlikely that the two lowest energy bands in $Fe_3(CO)_{12}$ are due to MLCT transitions.

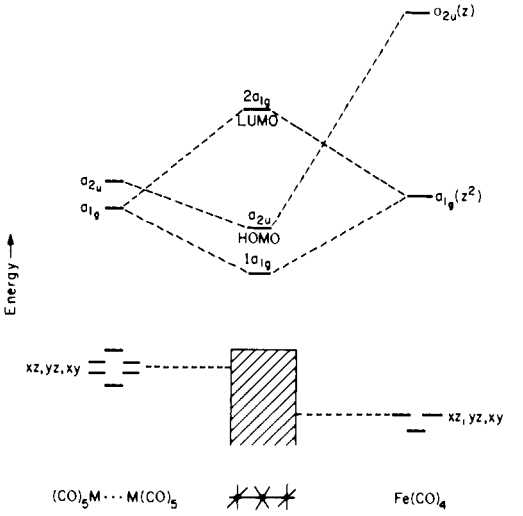

Figure 9. MO scheme for a D_{4h} $M_2Fe(CO)_{14}$ molecule.

Table III. Comparison of Band Positions in the Series $Fe_nRu_{3-n}(CO)_{12}$ (n = 0-3)

complex	$\sigma\rightarrow\sigma^*$, μm^{-1} ($\epsilon_M \times 10^{-4}$;[a] f[b])	$\sigma^{*\prime}\rightarrow\sigma^*$, ϵm^{-1} ($\epsilon_M \times 10^{-4}$;[a] f[b])
$Ru_3(CO)_{12}$	2.72 (1.02; 0.13)	3.12 (cannot be measured)
$FeRu_2(CO)_{12}$	2.72 (1.28; 0.18)	2.13 (0.70; 0.06)
$Fe_2Ru(CO)_{12}$	2.63 (0.86; 0.15)	1.79 (0.68; 0.07)
$Fe_3(CO)_{12}$	2.29 (0.48; 0.04)	1.66 (0.52; 0.08)

[a] 77 K. [b] Oscillator strength (f) as defined in ref 1.

It remains to assign the $\sigma\rightarrow\sigma^*$ and $\sigma^{*\prime}\rightarrow\sigma^*$ transitions in $Fe_3(CO)_{12}$. For this, a comparison of the spectra of the complexes in ther series Fe_nRu_{3-n} $(CO)_{12}$ (n = 0-3) is useful (Table III). We discussed above why the $\sigma^{*\prime}\rightarrow\sigma^*$ transition is lower in energy than $\sigma\rightarrow\sigma^*$ in $FeRu_2(CO)_{12}$. Upon substitution of another Fe for Ru to give $Fe_2Ru(CO)_{12}$, the $\sigma^{*\prime}\rightarrow\sigma^*$ transition should fall to even lower energy. Indeed, the lowest energy band is now at 1.79 μm^{-1} in comparison to 2.13 μm^{-1} in $FeRu_2(CO)_{12}$. The band is at lower energy still in $Fe_3(CO)_{12}$ (1.66 μm^{-1}). Thus, the $\sigma^{*\prime}\rightarrow\sigma^*$ transition energy decreases as the average splitting of the xz and z^2 orbitals decreases. The $\sigma\rightarrow\sigma^*$ transition is assigned to the 2.29-μm^{-1} band. This band is unresolved in solution at room temperature, so it is difficult to determine if the band blue shifts and sharpens on cooling. However, we note that the 1.66-μm^{-1} band red shifts on cooling, which indicates that a $\sigma\rightarrow\sigma^*$ transition is not involved.

Charge Transfer Bands

Metal to ligand charge transfer transitions in metal carbonyls generally fall in the ultraviolet region of the spectrum.[1] The energies of such transitions are mainly determined[1] by the nature of the central metal atom; i.e., the positions of d(Fe) $\rightarrow$ π^*CO and d(Ru) $\rightarrow$ π^*CO charge transfers in $Fe_3(CO)_{12}$ and $Ru_3(CO)_{12}$ may be reasonably estimated from the MLCT band energies observed for $Fe(CO)_5$ and $Ru(CO)_5$, respectively. The lowest MLCT band in the spectrum of $Fe(CO)_5$ falls at 242 nm (4.13 μm^{-1}),[24] whereas that in $Ru(CO)_5$ occurs at 236 nm (4.24 μm^{-1}) (Table II). Thus we assign the intense bands at 263 nm (3.80 μm^{-1}) in $Fe_3(CO)_{12}$ and at 238 nm (4.20 μm^{-1}) in $Ru_3(CO)_{12}$ to MLCT transitions. By analogy, the band at 240 nm (4.17 μm^{-1}) in the spectrum of $Os_3(CO)_{12}$ is attributed to a similar MLCT transition.

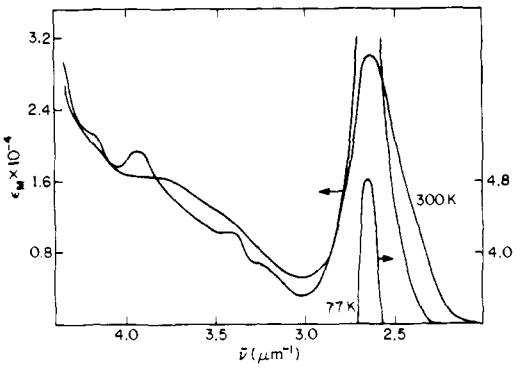

Figure 10. Electronic absorption spectra of $Re_2Fe(CO)_{14}$ in 3-PIP at 300 and 77 K.

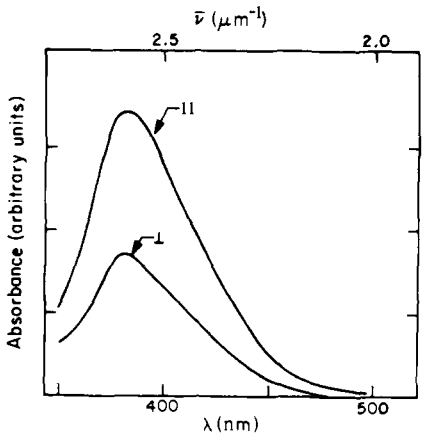

Figure 11. Polarized spectra of $Re_2Fe(CO)_{14}$ in BPC; the spectra are corrected for the absorption of BPC and are for the electric vector of light polarized parallel (||) and perpendicular (⊥) to the long axis of the oriented BPC molecules (see ref 12).

D_{4h} $M_2Fe(CO)_{14}$ Complexes

Figure 9 illustrates the proposed MO scheme for D_{4h}[25] $M_2Fe(CO)_{14}$-type (M = Mn, Re) molecules. If Z is taken as the internuclear axis, then metal-metal bonding is expected to involve mainly the d_{z^2} orbitals. The $3d_{z^2}$ orbital on Fe transforms as a_{1g}; thus, in the trinuclear molecule the Fe $3d_{z^2}$ interacts with the M_2 a_{1g} combination to form bonding and antibonding molecular orbitals. The M_2 a_{2u} combination is stabilized by interaction with the Fe $4p_z$ orbital.

The d_{xz}, d_{yz}, and d_{xy} orbitals, which are of π or δ symmetry in $M_2Fe(CO)_{14}$, lie to lower energy. As the overlaps between the π or δ orbitals on different metal atoms are small, these orbitals will lie below the d_{z^2} levels in the trinuclear molecules. The $d_{x^2-y^2}$ orbitals are strongly antibonding with respect to the CO donor orbitals; hence, they are higher in energy than the d_{z^2} levels. Thus, of the 22 d valence electrons in $M_2Fe(CO)_{14}$, 18 occupy the low-lying $d\pi$ and $d\delta$ orbitals, and the remaining 4 electrons fill the bonding a_{1g} and a_{2u} molecular orbitals. The ground state is $^1A_{1g}$ ($1a_{1g}^2 a_{2u}^2$).

The crystal structure determination[24] of $Mn_2Fe(CO)_{14}$ provides evidence that the mixing of the M_2 a_{2u} combination with the Fe $4p_z$ orbital is important. Without such interaction, the a_{2u} level would be nonbonding, implying weak metal-metal bonds relative to $Mn_2(CO)_{10}$. However, the MnFe bond length is 2.81 Å,[25] which is slightly *shorter* than the MnMn bond length of 2.92 Å in $Mn_2(CO)_{10}$.[26]

The lowest allowed electronic excitation is predicted to be $^1A_{1g} \rightarrow {}^1A_{2u}$ ($a_{2u} \rightarrow 2a_{1g}$), which is a $\sigma \rightarrow \sigma^*$ transition. This transition should be polarized along the MFeM(Z) axis. Note that the $1a_{1g} \rightarrow 2a_{1g}$ transition is not allowed. The spectra of $Re_2Fe(CO)_{14}$ at 300 and 77 K are shown in Figure 10. We have found that the lowest energy band in $Re_2Fe(CO)_{14}$ is polarized along the ReFeRe axis in the nematic liquid crystal solvent BPC (Figure 11). This finding is consistent with a $\sigma \rightarrow \sigma^*$ ($a_{2u} \rightarrow 2a_{1g}$) assignment for the band in question. A similar assignment is made for the intense lowest energy band in $Mn_2Fe(CO)_{14}$ (Table II). The $\sigma \rightarrow \sigma^*$ band in MnFeRe-$(CO)_{14}$ (2.48 μm^{-1}) falls between those of $Mn_2Fe(CO)_{14}$ (2.32 μm^{-1}) and $Re_2Fe(CO)_{14}$ (2.63 μm^{-1}).

The energy of the $a_{2u} \rightarrow 2a_{1g}$ band maximum increases by about 0.4 μm^{-1} in $Mn_2Fe(CO)_{14}$ on going from 300 to 77 K, whereas in $Re_2Fe(CO)_{14}$ it blue shifts 0.1 μm^{-1}. This characteristic behavior of a $\sigma \rightarrow \sigma^*$ band has now been demonstrated for $M_2(CO)_{10}$-,[1] $M_2(CO)_8$-,[23] $M_3(CO)_{12}$-, and $M_4(CO)_{12}$-[27] type compounds and their derivatives.

Acknowledgment. We thank David M. Dooley for assistance with certain of the MCD spectroscopic measurements. This research was supported by the National Science Foundation (CHE75-19086).

Supplementary Material Available: Listing of basis functions, eigenvectors, and eigenvalues for $Ru(CO)_4$ and $Ru_3(CO)_{12}$ (29 pages). Ordering information is given on any current masthead page.

References and Notes

(1) R. A. Levenson and H. B. Gray, *J. Am. Chem. Soc.*, **97**, 6042 (1975).
(2) M. S. Wrighton, *Top. Curr. Chem.*, **65**, 37 (1975).
(3) B. F. G. Johnson, J. Lewis, and M. V. Twigg, *J. Organomet. Chem.*, **67**, C75 (1974).
(4) M. I. Bruce, G. Shaw, and F. G. A. Stone, *J. Chem. Soc., Dalton Trans.*, 2094 (1972).
(5) J. P. Candlin and A. C. Shortland, *J. Organomet. Chem.*, **16**, 289 (1969).
(6) D. B. W. Yawney and F. G. A. Stone, *J. Chem. Soc. A*, 502 (1969).
(7) U. Anders and W. A. G. Graham, *Chem. Commun.*, 291 (1966).
(8) E. H. Schubert and R. K. Sheline, *Z. Naturforsch. B*, **20**, 1306 (1965).
(9) G. O. Evans and R. K. Sheline, *J. Inorg. Nucl. Chem.*, **30**, 2862 (1968).
(10) G. O. Evans, J. P. Hargaden, and R. K. Sheline, *Chem. Commun.*, 186 (1967).
(11) R. K. Sheline and K. S. Pitzer, *J. Am. Chem. Soc.*, **72**, 1107 (1950).
(12) R. A. Levenson, H. B. Gray, and G. P. Ceasar, *J. Am. Chem. Soc.*, **92**, 3653 (1970).
(13) L. F. Dahl and R. E. Rundle, *J. Chem. Phys.*, **27**, 323 (1957).
(14) N. A. Beach and H. B. Gray, *J. Am. Chem. Soc.*, **90**, 5713 (1968).
(15) R. Mason and A. I. M. Rae, *J. Chem. Soc. A*, 778 (1968). A redetermination of the $Ru_3(CO)_{12}$ structure was reported recently. See M. R. Churchill, F. J. Hollander, and J. P. Hutchinson, *Inorg. Chem.*, **16**, 2655 (1977). The small differences in reported bond angles and bond lengths should not affect the results significantly.
(16) B. J. Ransil, *Rev. Mod. Phys.*, **32**, 245 (1960).
(17) H. Basch and H. B. Gray, *Theor. Chim. Acta*, **4**, 367 (1966).
(18) A complete listing of eigenvalues and eigenvectors for $Ru(CO)_4$ and $Ru_3(CO)_{12}$ is available. See paragraph at end of paper regarding supplementary material.
(19) M. Elian and R. Hoffmann, *Inorg. Chem.*, **14**, 1058 (1975).
(20) E. R. Corey, Ph.D. Thesis, University of Wisconsin, 1963.
(21) (a) A. J. Deeming, B. F. G. Johnson, and J. Lewis, *J. Chem. Soc. A*, 897 (1970); (b) M. I. Bruce, G. Shaw, and F. G. A. Stone, *J. Chem. Soc., Dalton Trans.*, 2094 (1972).
(22) C. O. Quicksall and T. G. Spiro, *Inorg. Chem.*, **7**, 2365 (1968).
(23) H. B. Abrahamson, C. C. Frazier, D. S. Ginley, H. B. Gray, J. Lilienthal, D. R. Tyler, and M. S. Wrighton, *Inorg. Chem.*, **16**, 1554 (1977).
(24) M. Dartiguenave, Y. Dartiguenave, and H. B. Gray, *Bull. Soc. Chim. Fr.*, 4223 (1969).
(25) P. A. Agron, R. D. Ellison, and H. A. Levy, *Acta Crystallogr.*, **23**, 1079 (1967).
(26) L. F. Dahl and R. E. Rundle, *Acta Crystallogr.*, **16**, 491 (1963).
(27) D. R. Tyler and H. B. Gray, unpublished results.